



Effects of Substrate Roughness on Splat Formation for Ni-Cr Particles Plasma Sprayed onto Aluminum Substrates

S. Brossard, P.R. Munroe, A.T.T. Tran, and M.M. Hyland

(Submitted February 17, 2010; in revised form April 8, 2010)

Roughening of the substrate, for instance by grit-blasting or etching, is often used before plasma spraying in order to provide a high degree of roughness that promotes mechanical interlocking of the sprayed coating and consequently improved adhesion. This study investigates the morphology and microstructure of NiCr splats formed on such rough Al substrates, where roughness was generated by a number of methods including grinding and etching. Cross sections of the splats and the splat-substrate interface were examined using a range of electron microscopy techniques. Localized substrate melting and chemical mixing with the splat material was observed, forming very particular structures. The formation of various oxides phases and voids was also noted and found to increase, along with the degree of the substrate melting, with increasing substrate roughness. The structures observed were related to the spray conditions and substrate morphology.

Keywords aluminum, interface, nickel-chromium, plasma spray, roughness, splat

1. Introduction

Thermal spraying processes encompass a number of coating manufacturing techniques aimed at enhancing the performance of components or increasing their durability, while conserving the properties of the bulk substrate material. Among them, conventional plasma spraying makes use of a plasma jet to melt the particles, which are then sprayed, usually in a fully molten state, onto the substrate, flattening upon impact in lamellae often termed “splats,” which by accumulation end up creating a coating of a thickness generally around a few hundred microns in thickness (Ref 1-3).

The mechanical properties of the coatings depend heavily on the adhesion mechanisms between the first splats to form and the substrate (The adhesion between subsequent layers is, of course, also of importance). Many studies have investigated these mechanisms by studying single splats sprayed onto smooth substrates (Ref 4-7). In particular, it was noted that localized melting of the substrate from the heat provided by the sprayed particle may occur, which may then lead to the formation of intermetallic compounds or the generation of nonequilibrium microstructures (Ref 4, 8). In such cases, metallurgical

bonding is achieved, and assuming that the interfacial phase is not brittle, this is then beneficial for adhesion strength (Ref 1, 2). When substrate melting does not occur, as limited to certain spray conditions and combinations of materials, adhesion between splat and substrate may occur by either diffusion between the splat and substrate (Ref 9-11) or chemical-metallurgical interactions (Ref 12). Although it should be noted that this only occurs in zones where good contact is achieved, which are then often present in local regions of the substrate-coating interface due, for instance, to the presence of voids. However, in many cases, bonding is mechanical, occurring by interlocking between the splat and substrate (Ref 1). To obtain effective bonding plasma spraying is often performed onto rougher substrates, usually prepared by processes such as grit-blasting to promote such mechanical interlocking (Ref 1, 2, 13).

When discussing the effect of roughness on splat formation and adhesion to the substrate, Fauchais et al. made a distinction between cases of low roughness ($R_a < 2 \mu\text{m}$) and high roughness ($R_a > 2 \mu\text{m}$) (Ref 14). Some models and experiments showed that increasing substrate roughness, but keeping the roughness level below $2 \mu\text{m}$, resulted in decreasing the contact angle of the splat on the substrate, thus increasing splat thickness, decreasing flattening time and increasing the solidification time (Ref 15, 16). Other studies, on the other hand, found that wetting of the substrate was often improved (Ref 14), which may result in larger and flatter splats (Ref 11, 17, 18). These effects may also depend on the manner by which the increased roughness is achieved, notably if it is by preheating the substrate to oxidize its surface (Ref 14).

In the cases of higher roughness (i.e., $>2 \mu\text{m}$), however, the spreading of the splat may be hindered by irregularities present on the substrate surface (Ref 14, 19), especially if the wavelength (i.e., the distance between two

S. Brossard and P.R. Munroe, School of Materials, University of New South Wales, Sydney, NSW 2052, Australia; and A.T.T. Tran and M.M. Hyland, Chemical and Materials Engineering Department, University of Auckland, Auckland 1142, New Zealand. Contact e-mail: sophie.brossard@student.unsw.edu.au.

consecutive peaks) of these irregularities is smaller than the particle diameter (Ref 20). If it becomes greater than the particle diameter, Liu et al.'s model showed that spreading of the liquid droplet ends up in “violent” break up of the splat (Ref 20). Inducing such high roughness was then usually found to cause extensive finger formation in the splats (Ref 21, 22), but the adhesive strength may also be improved due to increased mechanical interlocking (Ref 13, 22). Furthermore, a reduction in the number of voids in the formed splat may occur, as found by Qu and Gouldstone who observed that micron-scale roughness may decrease the driving force for bubble nucleation and also prevent splat curling-up (Ref 23), a phenomenon often observed for splats formed on flatter substrates (Ref 24). However, numerical simulations showed that larger voids may form from the incomplete filling of the crevices of the surface by the splat material (Ref 25, 26).

Wroblewski et al. substrate (Ref 27) and Basu et al. substrate (28) studied by both experiments and modeling the influence of roughness on substrate melting upon spraying yttria-stabilized zirconia (YSZ) splats onto a YSZ substrate. They found that such melting occurred at a lower substrate heating temperature or, to a greater extent, for a lower roughness ($R_a = 50\text{--}100\text{ nm}$) than for a higher roughness levels (several microns). Both roughness levels were noted to be more prone to substrate melting than a smoother substrate.

It can be noted that for almost all the studies on the effects of surface roughness on splat formation, only the exterior morphology of the splats was observed. Xue et al. (Ref 25) and Parizi et al. (Ref 26) presented relatively low spatial resolution cross sections of splats on artificially patterned surfaces but did not include any chemical analysis of the phases present. In other studies, properties, such as the adhesion strength, were measured. Consequently, only very limited work has been published on the observation of cross sections of splats made on rough substrates ($R_a > 2\text{ }\mu\text{m}$), which could reveal, in detail, the structural and chemical interaction between the splat and substrate. This study, on the other hand, proposes to study the microstructure of splats, formed on substrates presenting various level of roughness, at a nano-scale level, using a range of electron microscopy techniques. NiCr particles, a material commonly used in plasma spray coating for applications such as bond coats or wear-resistant coatings (Ref 2), were then plasma sprayed onto aluminum substrates having undergone various pre-treatments to generate different levels of surface roughness. The results are compared with studies obtained for smoother substrates, which are described in more detail in an associated study (Ref 8).

2. Experimental Procedure

Five different substrates were used; prepared from either aluminum 1005 or 5052. [Details on both alloys, which differ in their Mg content (2.2–2.8 wt.% in Al5052, close to nil in Al1005), can be found in the associated

Table 1 Substrate nomenclature and condition

Specimen	Substrate	Pretreatment
Al5052_P	Aluminum 5052	Polished to a nanoscale roughness
Al1005_R	Aluminum 1005	Roughened with sand paper
Al1005_GB	Aluminum 1005	Grit blasted
Al5052_E	Aluminum 5052	Etched in HF
Al5052_ET	Aluminum 5052	Etched in HF and heat treated in air (350 °C, 90 min)

paper; Ref 8]. However, it was found that the difference in composition between both alloys did not have any significant influence on splat formation. The different substrates and their methods of preparation are listed in Table 1.

The polished substrates were mechanically ground and mirror polished with diamond paste, to a nanoscale roughness. The roughened substrate was ground using sand paper P120 (average particle diameter of 125 μm). The grit-blasted substrate was grit blasted with ICMAD-A BlastAB 14ED using a pressure of 50 psi for 2 min. Finally, the etched substrates were immersed at room temperature for 10 min in a solution made of 10% HF and 15% H_2SO_4 . One of them was then heat treated in air for 90 min at 350 °C.

The sprayed material was a commercial NiCr alloy powder (Ni80-Cr20, Sulzer Metco 43 VF-NS, Switzerland, $(-106+45)\text{ }\mu\text{m}$). Plasma spraying was carried out with a Sulzer Metco (Switzerland) 7 MB gun (with a nozzle diameter of 8 mm), operating at a current of 550 A and at a voltage of 62 V, with a spraying distance of 100 mm (the injector had a diameter of 1.8 mm and was at an angle of 90° with the substrate surface). The feeding rate of the powder was of 1 g/min, the carrier gas being argon at a flow rate of 3 SLPM, while the plasma gas was a mixture of nitrogen and hydrogen, at a flow rate of 47.5 SLPM and 6.2 SLPM, respectively. The measured temperature and velocity of the sprayed particles were $\sim 2450\text{ }^\circ\text{C}$ and $\sim 115\text{ m s}^{-1}$, respectively, meaning that the particles were fully molten upon impact (the melting point of NiCr is 1400 °C; Ref 29).

The specimens were then characterized using a range of analytical techniques. A scanning electron microscope (SEM) (Hitachi, S3400-X, Mito, Japan) was used to image the overall morphology of the splats and the substrates. A focused ion beam microscope (FIB) (FEI, xP200, Hillsboro, USA) was used to mill cross sections of the splats using an energetic gallium ion beam, and to image them using secondary electrons induced by the ion beam. Details have been described elsewhere (Ref 30). A dual beam microscope (that is a FIB and SEM combined into a single instrument) (FEI, xT Nova Nanolab 200, Hillsboro, USA) was used to prepare cross sections of splats (100–200 nm in thickness) suitable for TEM observation. These were prepared using the lift-out method as described elsewhere (Ref 30) and examined in a transmission electron microscope (TEM) (Philips, CM200, Eindhoven, The Netherlands) to which energy dispersive x-ray spectroscopy (EDS) facilities have been interfaced. Finally, the average surface roughness of the substrates was assessed using an atomic force microscope (AFM)

(Digital Instruments DI3000, Santa Barbara, CA), except for the very rough substrates (A11005_R and A11005_GB), whose roughness was evaluated using a profilometer (Mitutoyo Surfpak-SV 600, Aurora, CO).

Several FIB and TEM cross sections were prepared and studied for each particular feature and/or type of splat. However, for reasons of brevity only a small number of representative images will be presented here. The cross section preparation process using FIB also involves the deposition of a layer of platinum on top of it prior to milling for protection purposes. This layer is present on the FIB and TEM images presented.

3. Results and Discussion

The morphology and microstructure of the typical splats found on the different substrates will be described from the observations made from the electron microscope images and cross sections. Once they are described, the formation of the various features observed will be discussed.

3.1 Splat Microstructure and Formation on the Polished Substrates

In an associated paper by the same authors (Ref 8), the morphology, microstructure, and formation process of NiCr splats plasma sprayed onto aluminum substrates were described. This includes both Al5052 and Al1005 alloys, having first undergone polishing to nanoscale levels of roughness, and in some cases, thermal pretreatments aimed at modifying the substrate surface chemistry. The observations made are briefly summarized here to allow comparison with the rougher substrates described in more detail in this paper.

Figure 1 presents two SEM images of the most typical splat morphologies found on polished Al5052 (roughness $R_a = [7.3 \pm 2.3]$ nm). For the larger splat with a ring of splashed fingers (Fig. 1a), evidence of localized substrate melting was found at the splat-substrate interface toward the center of the splat, along with chemical mixing between the NiCr and Al phases, forming some interfacial layers of both a metastable metallic glass and a very fine mixture of Ni and Al nonequilibrium phases, associated

with the rapid solidification of the melted phases. This structure was also found to form on substrates with a higher roughness, as will be described later in detail.

The splat shown in Fig. 1(b), however, displayed no, or very few, splashed fingers. For these splats, as well as for the splats with a ring of splashed fingers toward their periphery, the splat-substrate interface was typically found to be straight and distinct, often with a poor contact between splat and substrate. Voids and various oxides phases, such as alumina $\gamma\text{-Al}_2\text{O}_3$, Cr_2O_3 , or spinel-like NiAl_2O_4 , were found to form in typical locations around the splat. It was also found that effects of heat treating the substrate prior spraying, or using an alloy containing or not containing Mg (Al5052 compared to Al1005), had negligible effects on the splat morphology. As noted earlier, more details of these structures can be found elsewhere (Ref 8).

In addition, other types of splats were observed, such as the splats without a ring of splashed fingers, as shown in Fig. 1(b), and presented a similar structure as the one described above, except no evidence of substrate melting was usually found: the splat-substrate interface was mostly distinct and straight. Evidence of a slower solidification rate (poorer contact at the interface, coarser grain structure) and larger concentration of oxides were also observed.

3.2 Splat Microstructure and Formation for the Roughened and Grit-Blasted Substrates

As it can be observed in Fig. 2(a), when examining the substrate surface around the splat, the roughened substrate displays many scratches from the grinding process. The surface roughness was measured to be $R_a = [1.2 \pm 0.2]$ μm . On the other hand, the grit-blasted substrate (Fig. 2b) displays cavities and peaks which are less linear compared to the elongated scratches on the ground substrate. The average roughness is also significantly higher ($R_a = [6.9 \pm 0.2]$ μm).

Figure 2 shows SEM images of splats found on Al1005_R (Fig. 2a) and Al1005_GB (Fig. 2b): both appear irregularly shaped, with some spherical particles distributed around the splat. As it can be seen on the FIB cross sections presented in Fig. 3, made on various

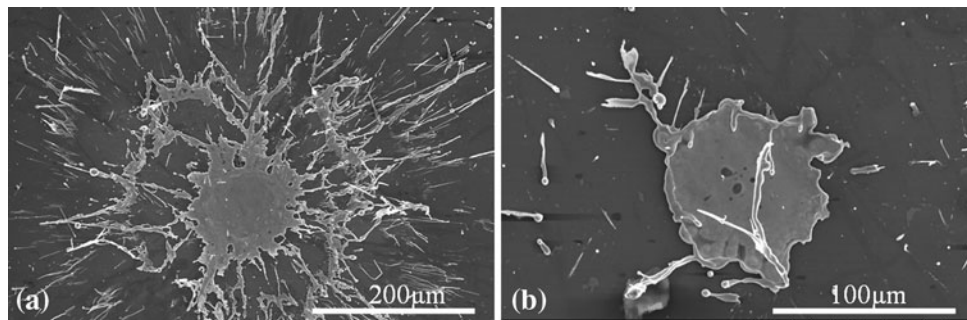


Fig. 1 SEM images of typical splats found on Al5052_P

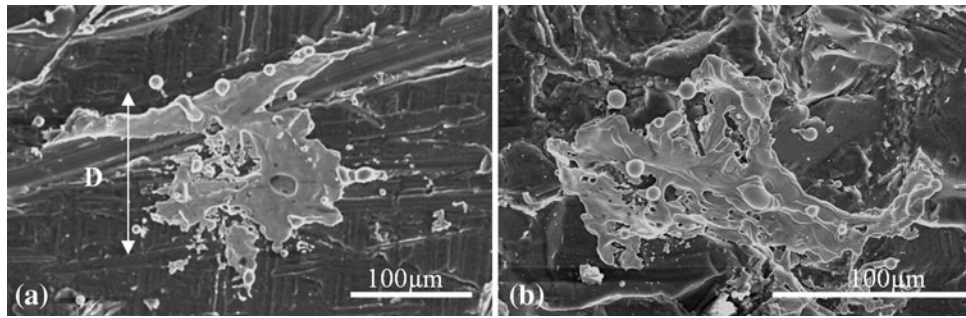


Fig. 2 SEM images of typical splats found on (a) Al1005_R and (b) Al100_GB

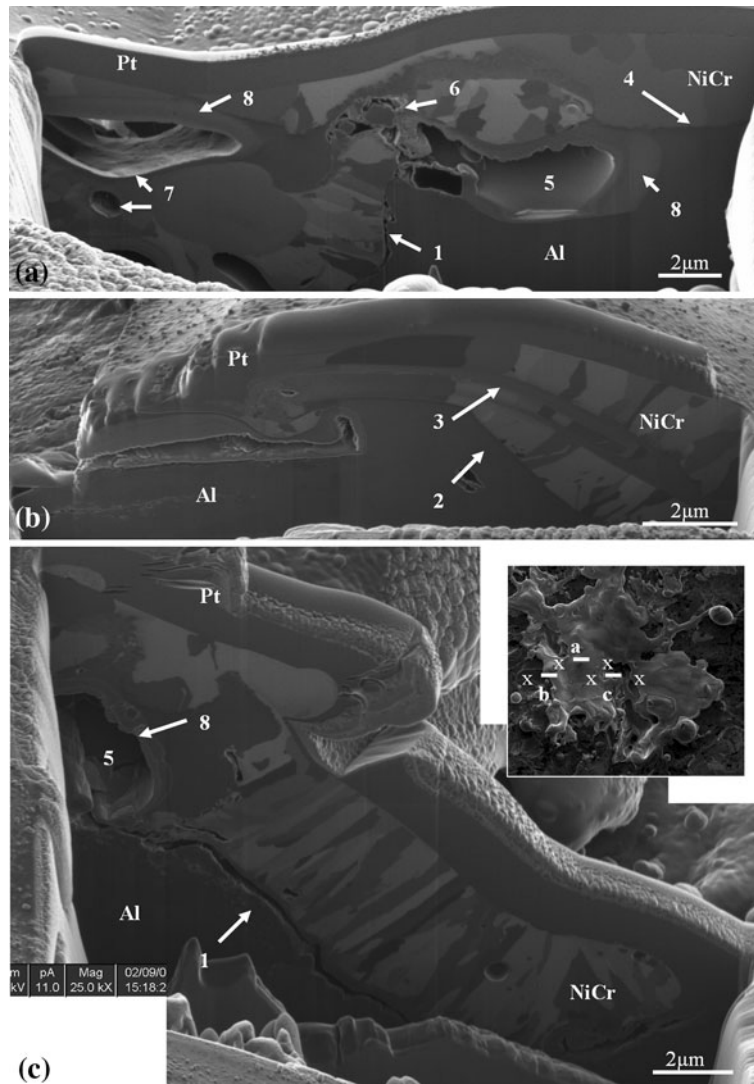


Fig. 3 FIB cross sections made across various locations on a splat (see inset image) found on Al1005_GB

locations across a splat on Al1005_GB, the microstructure of such a splat is very irregular. In some zones, such as the ones marked 1 on Fig. 3(a) and (c), the contact between the splat and substrate is poor, and the splat-substrate

interface is irregularly shaped, as seen for instance in Fig 3(b) (marked 2). In contrast, in some regions the contact between both phases is excellent and evidence of localized substrate melting can be observed. Indeed,

jetting of Al within the NiCr phase can be seen (marked 3), which can only have formed from the melting of the substrate and mixing of the latter with the flowing molten splat. Finally, in other locations the contact between splat and substrate interface appears good (marked 4 on Fig. 3a), but as it is not clear if the irregular shape of the interface arises from the original substrate topography or from localized melting and mixing of the substrate, it cannot be definitely concluded whether substrate melting has occurred or not.

However, when substrate melting does occur, a distinctive interfacial structure may form, as it can be observed on the TEM cross section presented in Fig. 4. Toward the right side of the section, the contact between splat and substrate is good and the interface appears

indistinct on the bright field image (see 1 on Fig. 4a). The EDS elemental linescan L1, performed across the interface, reveals a gradual variation of the concentrations in Ni and Al (2), showing that mixing between both phases has occurred over a depth of about 400 nm. The fact that these variations do not exhibit a step-function shows that there is no defined stoichiometric intermetallic compound present at the interface. However, on the higher magnification bright field image of the interface, two layers can be seen: a first layer close to the splat which appears featureless (3), and a second layer of nanosized grains with needle-like shape normal to the interface (4). This particular interfacial structure was observed for the polished substrates and described in more detail in the associated paper (Ref 8). It was concluded that the first layer was a

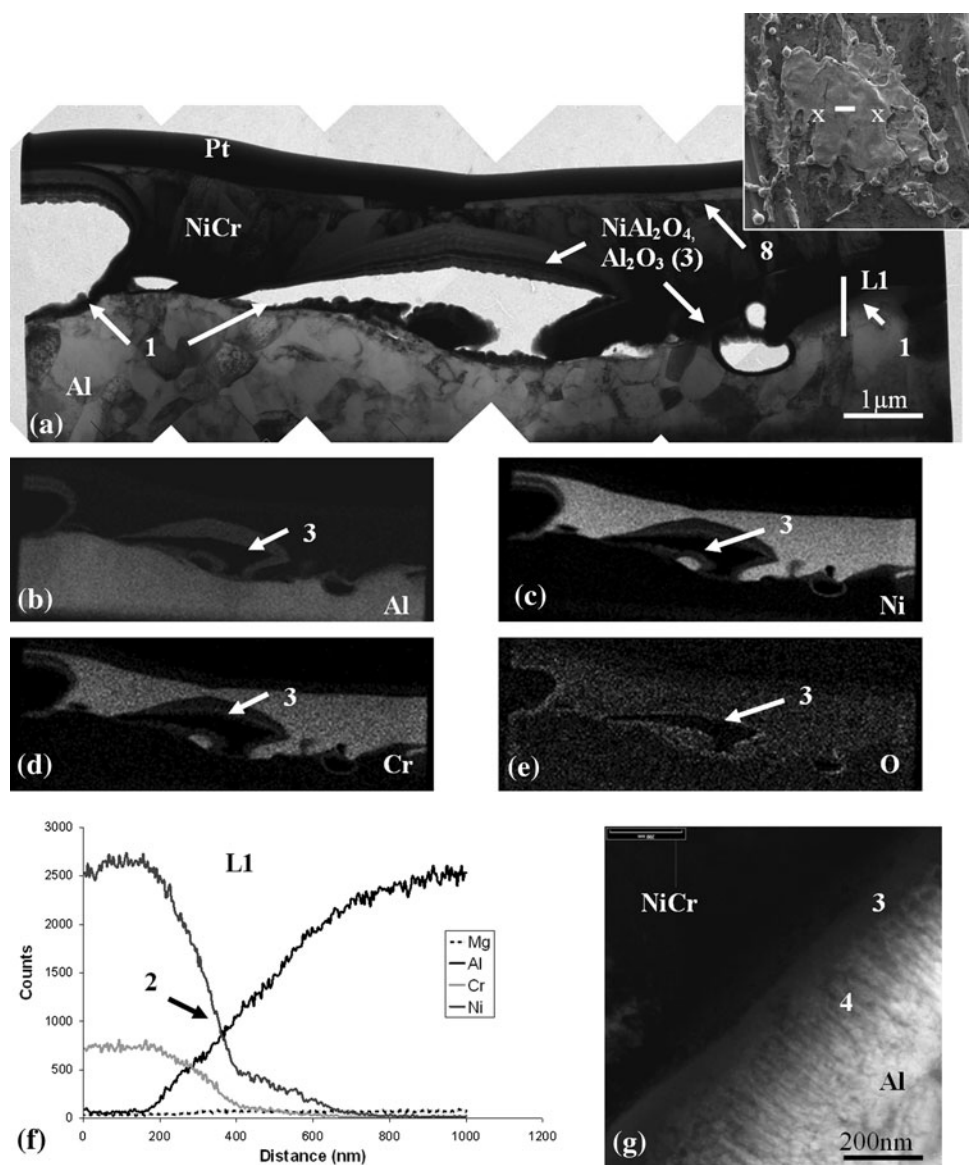


Fig. 4 TEM cross section across a splat (see inset image) found on Al1005_R: (a) bright field image, EDS elemental maps for (b) Al, (c) Ni, (d) Cr, (e) O, (f) EDS elemental linescan, (g) high-magnification bright field image of the splat-substrate interface

metastable metallic glass composed of a mixture of Al and NiCr, while the second layer was a mixture of nanosized Ni-rich and Al-rich metastable phases. Also, any possible oxide layer present on the substrate surface prior to spraying (Ref 31) must have been removed upon splat formation, as it could not be observed here at the splat-substrate interface.

Large voids (several microns in size) can be found to have formed near the splat-substrate interface (see 5 on Fig. 3a and c), along with some much smaller ($<1\ \mu\text{m}$ in size) voids (for instance 6 on Fig. 3b), also within the splat itself (see 7 on Fig. 3a). Especially visible for the larger voids are thick and dense oxide layers that can be observed on the walls of most voids (for instance 8 on Fig. 3a and c). Studies of the oxidation of alloys containing Al, Ni, and Cr showed that alumina $\gamma\text{-Al}_2\text{O}_3$, chromium oxide Cr_2O_3 , NiO, and spinel species such as NiAl_2O_4 and NiCr_2O_4 were the most probable oxides to form (Ref 32). On the TEM cross section shown in Fig. 4, it can be seen from the EDS elemental maps (Fig. 4b-e) that on the walls of the large void present at the splat-substrate interface are oxide layers not only containing mainly Al, but also containing some Cr and Ni. The diffraction patterns of phases such as $\gamma\text{-Al}_2\text{O}_3$, NiO and spinels NiAl_2O_4 , and NiCr_2O_4 are all quite similar to each other (these phases have similar d -spacings) and are consistent with the patterns obtained from this area. However, from the EDS maps (3), it can be concluded that such layers may be composed mainly of alumina and a mixture of spinel (NiAl_2O_4 and/or NiCr_2O_4). Chromium oxide, notably Cr_2O_3 , was often reported to form as a thin dense layer on top of NiCr splats in previous studies (Ref 5, 8). Here, it was not observed on the TEM cross sections prepared; however, the possibility of its formation on other splats should not be ruled out.

Structural features, such as the presence of layers of Al folded within the splat (as seen in Fig. 3b) and voids located for instance within the splat, denote the chaotic spreading of the splat upon its formation. Many studies have reported that the presence of high-scale roughness-induced instabilities in the spreading of plasma-sprayed splat, causing the formation of features such as splashed fingers or voids (Ref 14, 20-22). The presence of hot oxidizing gases is also evident by the presence of layers of oxides observed on the walls of the voids. Such gases may come from desorption of adsorbates/condensates initially present on the surface of the substrate (Ref 33-35), or may have been entrapped in the cavities on the substrate surface upon particle impact and spreading (Ref 19), or finally, as suggested by Qu et al., they may come from gases that get dissolved within the molten particle due to the pressure upon impact, and which get released by the forming void due to the nucleation sites provided by the irregularities of the substrate's surface (Ref 23). However, it can be noted that some voids are significantly large (several microns in diameter), apparently too large to be formed solely from bubble formation. Several modeling studies of splat formation on flat surfaces have shown that large central voids may form due to the mechanics of the flow of the molten splat, because of the change in the

curvature of the droplet (Ref 36, 37). Also, other studies showed how voids can form from the incomplete filling of the crevices of the surface by the molten splat material (Ref 25, 26).

Localized melting of the aluminum substrate from the heat provided by the impacting molten NiCr particle was observed and was discussed in detail for polished substrates (Ref 8). Here, the presence of a large-scale roughness means that the molten flowing NiCr encounters peaks on the aluminum substrate, which are then prone to melting from both the heat and the pressure applied by the spreading splat. Previous studies showed that melting was more prominent for substrates with a large-scale roughness compared to smooth substrates. In addition to the mechanical interlocking induced by the irregularities of the substrate's surface, the metallurgical bonding that results from the melting of the substrate and intermixing with the splat material may be another factor contributing to the significant improvement in the adhesion strength usually observed for the coatings sprayed onto rougher specimens (Ref 13, 22). This is true, however, only if the interfacial phases formed are not brittle, which may not be the case for the glassy layer observed here (metallic glasses have very low ductility; Ref 38). Finally, a remark can be made about how the grit-blasted substrate Al1005_GB may present a higher adhesion strength compared to the rough substrate, Al1005_R, as the latter presents long scratches on its surface, while Al1005_GB exhibits more equiaxed anchorage points.

3.3 Splat Microstructure and Formation on the Etched and Etched and Thermally Treated Substrates

The etching treatment of the aluminum substrates produced many relatively small surface cavities (usually less than a few microns in size), as it can be observed when examining at the substrate surface around the splats in Fig. 5(a, b). The roughness levels measured were $R_a = [444 \pm 100]$ nm for the non-heat-treated substrate, and $R_a = [626 \pm 88]$ nm for the heat-treated substrate.

On Fig. 5 are displayed SEM images of typical splats found on both etched substrates, Al5052_E and Al5052_ET. In many instances, splats were found to be very fragmented as shown for example in Fig. 5(a), suggesting that the sprayed particle did not adhere to the substrate, leaving only some small droplets, many of which are spherical in morphology. This splat shape probably arises from surface tension effects (Ref 14). Figure 6 displays a FIB cross section performed across such a droplet. The very rounded splat shape can be noted (1), the grains are elongated in a direction normal to the interface (2), suggesting a slow solidification which can be linked to poor contact with the substrate (3).

As shown in the SEM image (Fig. 5b), the other splats were found to have a relatively irregular shape, although to a lesser extent compared to the splats found on the rough and grit-blasted substrates. Figure 7 displays FIB cross sections made across such a splat on the Al5052_ET substrate. The substrate surface is quite irregularly shaped

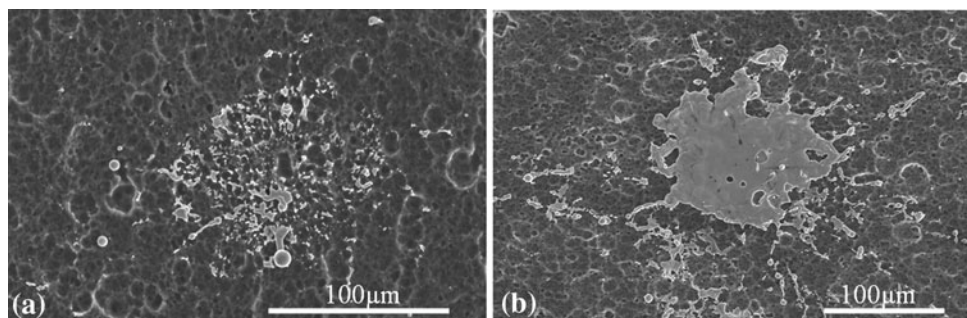


Fig. 5 SEM images of typical splats found in (a) Al5052_E and (b) Al5052_ET

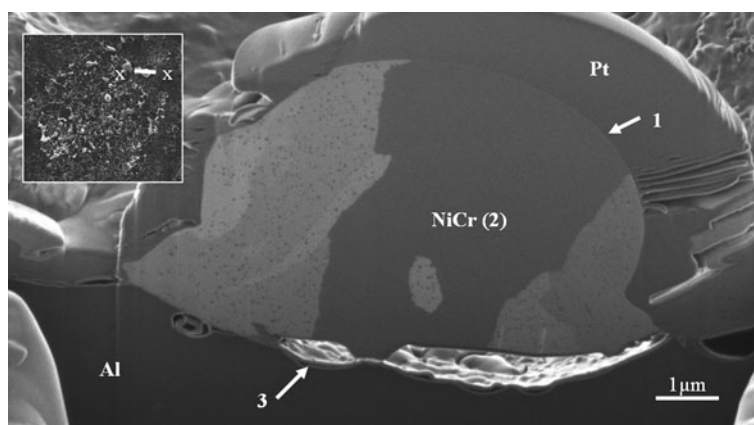


Fig. 6 FIB cross section of a NiCr droplet from a nonadhered splat (see inset image) found on Al5052_E

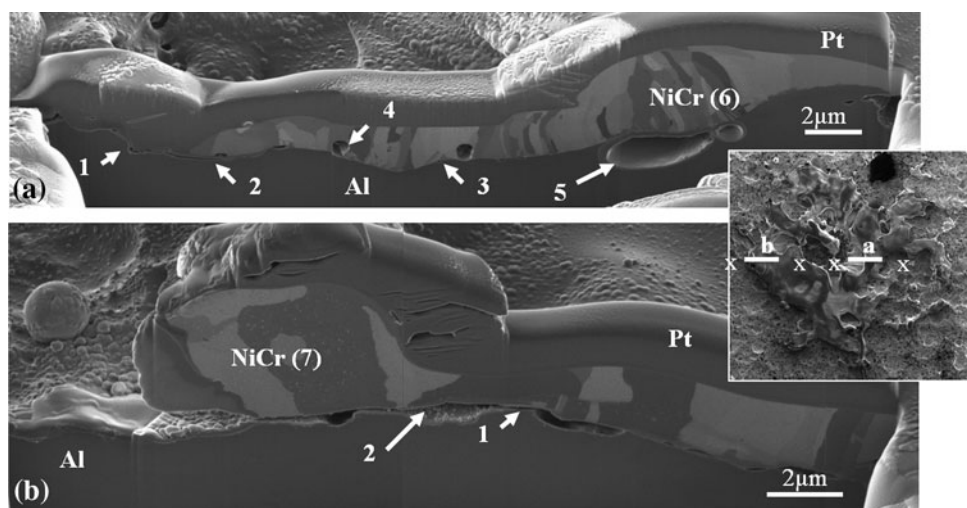


Fig. 7 FIB cross sections made across a splat (see inset image) found on Al5052_ET

(1), and the contact between splat and substrate is poor in some regions (2), while good in others (3). Voids can also be noted close to the interface, some within the splat (4), and some within the substrate (5). The voids, along with the irregularities of the substrate's surface, may have form either from localized substrate melting, as it has been

observed for the rough and grit-blasted specimens, or also may be due to the etching treatment. NiCr grains are quite irregularly shaped, often elongated in a normal direction to the interface in zones where there is good contact (6), showing the direction of solidification as the heat is efficiently removed through the interface. Where the contact

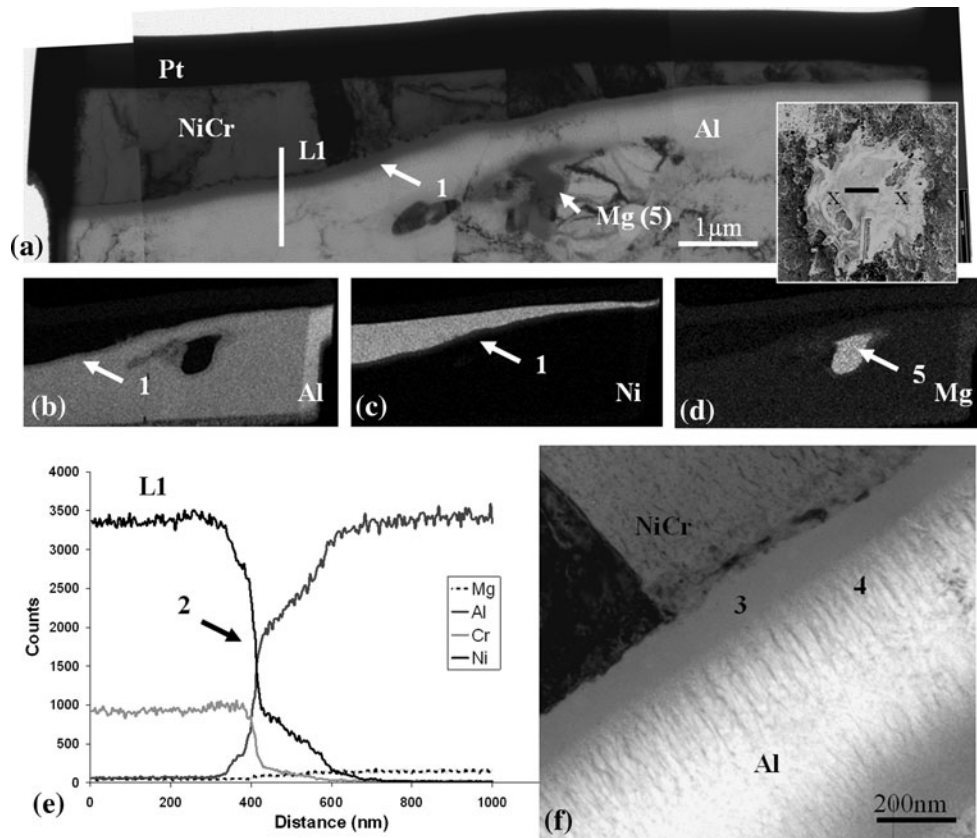


Fig. 8 TEM cross section across a splat (see inset image) found on Al5052_E: (a) bright field image, EDS elemental maps for (b) Al, (c) Ni, (d) Mg, (e) EDS elemental linescan, (f) high-magnification bright field image of the splat-substrate interface

is poor the grains are coarser (7) as the heat removal and solidification were slower and not as unidirectional because of the interfacial thermal contact resistance.

However, evidence of substrate melting was found, as for instance on the TEM cross section presented (Fig. 8). As it can be seen, the same distinct structure, as observed previously in zones of substrate melting for the polished and roughened specimen, is present here: the splat-substrate surface is quite indistinct (1); the EDS elemental linescan L1 performed across this interface (Fig. 8e) confirms the mixing between the NiCr and Al phases (2); on the higher magnification bright field image (Fig. 8f), the glassy layer (3) and the nanosized grained layer (4), discussed earlier, can be seen. Consequently, localized substrate melting, mixing with the splat material, and rapid solidification resulting in the formation of metastable phases (Ref 8) occurs on the etched substrates. The darker zone presents within the substrate that can be observed on the bright field image (Fig. 8a) was identified by EDS as being a Mg-rich intermetallic particle (5 on Fig. 8d).

The same range of oxide phases, as described earlier, was also present. For example, several oxide species were identified on the TEM cross section presented in Fig. 9. On the wall of the large voids, a thick and dense layer of alumina γ -Al₂O₃ can be seen (1) which was identified by elemental EDS mapping and electron diffraction (more details can be found on the identification of such phases in

an associated paper; Ref 8). A thin and dense layer of Cr oxide is present on top of the splat (2) which was identified as being Cr₂O₃. Toward the right side of the section, Cr₂O₃ is also found as a thicker, but less dense layer (3). Such a layer, which was also found to form similarly in irregularly shaped splats found on the polished substrates (see associated paper, Ref 8), may come from in-flight oxidation of the NiCr particle, a phenomenon that has been reported before in plasma spraying (Ref 33), or from oxidation occurring upon splat formation similarly as for the oxides formed in voids, which is, however, less likely (Ref 8).

Effects of a thermal treatment prior to plasma spraying on the substrate surface chemistry, roughness, and splat formation, were discussed in previous papers (Ref 8, 39). In summary, it was found that such heat treatment increased the γ -Al₂O₃ content of the oxide layers already present on the surface, partially dehydrating them (reducing the hydroxide content), and increasing the thickness (a few nanometers), and roughness (slightly from about 7 to 8 nm). Such changes had, however, limited effects on splat morphology and formation. However, in the case here of etched specimens, it was found that the proportion of “normal” splats, such as those seen in Fig. 5(b), compared to ensemble of small droplets resulting from the nonadhesion of the sprayed NiCr particle, such as seen in Fig. 5(a), was significantly increased by the heat treatment. That is, on Al5052_E there was around 3/4

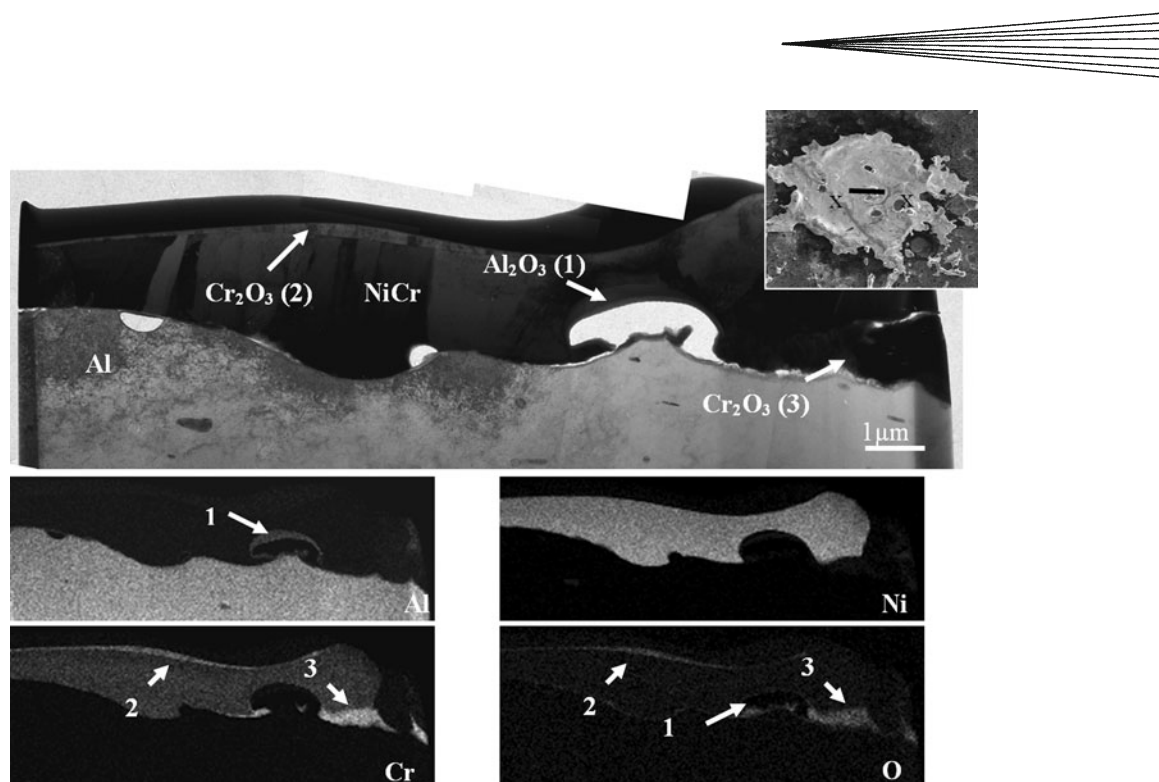


Fig. 9 TEM cross section across a splat (see inset image) found on Al15052_ET: (a) bright field image, EDS elemental maps for (b) Al, (c) Ni, (d) Cr, (e) O

of nonadhered splats and 1/4 of fully adhered splats, while on Al15052_ET all the splats found had fully adhered. The nonadhesion of sprayed particles on the etched substrate may itself be related to the etching treatment, which is performed by immersing the substrate in an acidic solution, since, even if it may be expected that the substrate would fully dry prior to spraying, it is likely that some chemical residues remain adsorbed onto the substrate surface, particularly considering the many cavities induced by the etching treatment. These are then likely to evaporate upon heating. This would then result in the release of a large amount of gas upon impact and spreading of the sprayed NiCr particle because of the heat, forming a gas cushion hindering the adhesion of the forming splat. On the other hand, heat treatment of the substrate would allow most of these adsorbed species to evaporate from the substrate surface, allowing a good adhesion of the sprayed particles on the substrate.

3.4 Effects of the Substrate Roughness on the Splat Formation Process

In Table 2 are detailed the average surface roughness measured for the different specimens studied, as well as the average diameters of the splats. Diameters, D , were evaluated for each splat by measuring the smallest and largest values and taking the average (see for instance, Fig. 2a), ignoring possible splashed fingers. Considering the very irregular shape of the splats, such measurements are approximate.

The roughness criteria used by Fauchais et al. stated that for $Ra < 2 \mu\text{m}$ the roughness is defined as “low”,

Table 2 Average roughness and average splat diameters for the different specimens

Specimen	Average roughness	Average diameter of the splats
Al15052_P	$Ra = [7.3 \pm 2.3] \text{ nm}$	$D = [89 \pm 38] \mu\text{m}$
Al11005_R	$Ra = [1.2 \pm 0.2] \mu\text{m}$	$D = [116 \pm 42] \mu\text{m}$
Al11005_GB	$Ra = [6.9 \pm 0.2] \mu\text{m}$	$D = [118 \pm 39] \mu\text{m}$
Al15052_E	$Ra = [444 \pm 100] \text{ nm}$	$D = [114 \pm 46] \mu\text{m}$
Al15052_ET	$Ra = [626 \pm 88] \text{ nm}$	$D = [114 \pm 24] \mu\text{m}$

and for $Ra > 2 \mu\text{m}$, it is defined as being “high” (Ref 14). With such a criteria, only the grit-blasted specimen would be considered high roughness. However, the microstructure of the splats observed for all four rough specimens (Al11005_R, Al11005_GB, Al15052_E, and Al15052_ET) appears to correspond to the effects described for surfaces which exhibit a high roughness, that is disturbance of the flow of the spreading molten splat by the irregularities of the interface (Ref 14, 19), creating very irregularly shaped splats (Ref 20-22), occurrence of substrate melting (Ref 27, 28), especially for the peaks of the surface, etc. Accurate quantification of the effects is difficult because of the relatively limited number of FIB and TEM cross sections that were prepared for each specimen. However, it can be noted that the etched specimens, in addition to presenting a relatively low roughness compared to the rough and grit-blasted ones, presented the most “regularly” shaped splats. However, less substrate melting was observed, which is in agreement with the observations made by Basu et al. and Wroblewski et al. (Ref 27, 28), together with less mixing with NiCr, and fewer and smaller

voids. It can also be noted that for the splats formed on rough surfaces, there is no sign of splashing in the way observed for smooth substrates (Ref 8), creating dense rings of splashed fingers (see Fig. 1a).

Roughening of the substrates is very often used in plasma spray to increase the adhesion strength of the coatings. Nevertheless, such a process may result in the formation of many large voids and significant concentrations of oxides compared to smoother substrates, which can be subsequently detrimental for some properties of the coating such as density, strength, thermal, and electrical conductivity. Moreover, while the adhesion strength increase observed is accounted to mechanical interlocking, here it was shown that on both smooth and rough substrates, the occurrence of substrate melting allowed metallurgical bonding to occur. On the other hand, there is the possibility that the glassy phase, associated with rapid solidification of the molten zone, found at the splat-substrate interface is brittle, which would then be detrimental to the quality of the metallurgical bonding. When intending to perform roughening of the substrate prior to spraying, it may be interesting to aim for an intermediate value for the roughness ($R_a = 0.5\text{--}1\ \mu\text{m}$), where mechanical interlocking would occur, but without resultant large voids and/or oxide formation.

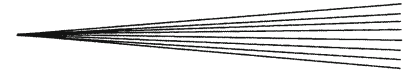
4. Conclusion

In summary, the following observations and conclusions can be drawn from the study by electron microscopy of the NiCr splats plasma sprayed onto Al substrates with various levels of roughness:

- The peaks and cavities present on the rough substrates hindered the spreading of the molten splats, leading to very irregular splat morphologies and the formation of many voids, including some very large voids (several microns in diameter).
- Localized substrate melting was observed for all smooth and rough substrates, notably for the peaks present on the rough ones. This led to mixing with the molten NiCr and the formation of metastable interfacial layers, including a metallic glass one which could potentially be detrimental to the adhesion strength of the coating.
- The formation of various oxide phases was observed. Their presence in some of the voids near the splat-substrate interface accounted for the release of gas from the substrate and/or the splat.
- Finally, it was noted that increasing the roughness resulted in an increase in the degree of substrate melting and the concentration of oxides and voids.

References

1. M. Dorfman, Thermal Spray Basics, *Adv. Mater. Process.*, 2002, **160**(7), p 47-50
2. R.F. Bunshah, *Handbook of Hard Coatings. Deposition Technologies, Properties and Applications*, Noyes Publications, William Andrew Publishing, Norwich, NY, 2001
3. M. Dorfman, Thermal Spray Processes, *Adv. Mater. Process.*, 2002, **160**(8), p 47-49
4. S. Kitahara and A. Hasui, A Study of the Bonding Mechanism of Sprayed Coatings, *J. Vac. Sci. Technol.*, 1974, **11**(4), p 747-753
5. S. Brossard, P.R. Munroe, A.T.T. Tran, and M.M. Hyland, Study of the Microstructure of NiCr Splats Plasma Sprayed on Stainless Steel by TEM, *Surf. Coat. Technol.*, 2009, **204**(9-10), p 1608-1615
6. H. Zhang, X.Y. Wang, L.L. Zheng, and X.Y. Jiang, Studies of Splat Morphology and Rapid Solidification During Thermal Spraying, *Int. J. Heat Mass Trans.*, 2001, **44**, p 4579-4592
7. L. Li, X.Y. Wang, G. Wei, A. Vaidya, H. Zhang, and S. Sampath, Substrate Melting During Thermal Splat Quenching, *Thin Solid Films*, 2004, **468**, p 113-119
8. S. Brossard, P.R. Munroe, A.T.T. Tran, and M.M. Hyland, Examination of the Splat Microstructure, Splat-Substrate Interface and the Effects of Substrate Heating on the Splat Formation for Ni-Cr Particles Plasma Sprayed onto Aluminum Substrates, Submitted to *J. Therm. Spray Technol.*, 2010. doi:10.1007/s11666-010-9511-2
9. V. Pershin, M. Lufitha, S. Chandra, and J. Mostaghimi, Effect of Substrate Temperature on Adhesion Strength of Plasma-Sprayed Nickel Coatings, *J. Therm. Spray Technol.*, 2003, **12**(3), p 370-376
10. S. Brossard, P.R. Munroe, and M.M. Hyland, Study of the Splat Formation for HVOF Sprayed NiCr on Stainless Steel Substrates and the Effects of Heating and Boiling Pre-treatments, *J. Therm. Spray Technol.*, in publication, 2010. doi:10.1007/s11666-010-9502-3
11. S. Brossard, P.R. Munroe, A.T.T. Tran, and M.M. Hyland, Study of the Effects of Surface Chemistry on Splat Formation for Plasma Sprayed NiCr onto Stainless Steel Substrates, *Surf. Coat. Technol.*, 2009, **204**(9-10), p 1599-1607
12. H.-D. Steffens, B. Wielage, and J. Drozak, Interface Phenomena and Bonding Mechanism of Thermally-Sprayed Metal and Ceramic Composites, *Surf. Coat. Technol.*, 1991, **45**, p 299-308
13. T. Chraska and A.H. King, Effect of Different Substrate Conditions Upon Interface with Plasma Sprayed Zirconia—A TEM Study, *Surf. Coat. Technol.*, 2002, **157**, p 238-246
14. P. Fauchais, M. Fukumoto, A. Vardelle, and M. Vardelle, Knowledge Concerning Splat Formation: An Invited Review, *J. Therm. Spray Technol.*, 2004, **13**(3), p 337-360
15. Z.G. Feng, M. Domaszewski, G. Montavon, and C. Coddet, Finite Element Analysis of Effect of Substrate Surface Roughness on Liquid Droplet Impact and Flattening Process, *J. Therm. Spray Technol.*, 2002, **11**(1), p 62-68
16. C. Moreau, P. Gougeon, and M. Lamontagne, Influence of Substrate Preparation on the Flattening and Cooling of Plasma-Sprayed Particles, *J. Therm. Spray Technol.*, 1995, **4**(1), p 25-33
17. J. Cedelle, M. Vardelle, B. Pateyron, and P. Fauchais, Investigation of Plasma Sprayed Coatings Formation by Visualization of Droplet Impact and Splashing on a Smooth Substrate, *Trans. Plasm. Sci.*, 2005, **33**(2), p 414-415
18. M. Raessi, J. Mostaghimi, and M. Bussmann, Effect of Surface Roughness on Splat Shapes in the Plasma Coating Process, *Thin Solid Films*, 2006, **506-507**, p 133-135
19. L. Bianchi, A.C. Leger, M. Vardelle, A. Vardelle, and P. Fauchais, Splat Formation and Cooling of Plasma-Sprayed Zirconia, *Thin Solid Films*, 1997, **305**, p 35-47
20. H. Liu, E.J. Lavernia, and R.H. Rangel, Modeling of Molten Droplet Impingement on Non-Flat Surface, *Acta Met. Mater.*, 1995, **43**(5), p 2053-2072
21. M. Ivošević, V. Gupta, J.A. Baldoni, R.A. Cairncross, T.E. Twardowski, and R. Knight, Effect of Substrate Roughness on Splating Behavior of HVOF Sprayed Polymer Particles: Modelling and Experiments, *J. Therm. Spray Technol.*, 2006, **15**(4), p 725-730
22. N. Ferguen, P. Fauchais, A. Vardelle, and D. Gobin, Numerical Investigation of Impact and Solidification of YSZ Droplets Plasma-Sprayed onto a Substrate: Effect of Thermal Properties and Roughness, *32nd International Conference on Advanced Ceramics and Composites*, H.-T. Lin and D. Zhu, Ed., January 27-February 1 (Daytona Beach, Florida, USA), The American Ceramic Society, p 159-170



23. M. Qu and A. Gouldstone, On the role of bubbles in metallic splat nanopores and adhesion, *J. Therm. Spray Technol.*, 2008, **17**(4), p 486-494
24. M. Xue, S. Chandra, and J. Mostaghimi, Investigation of Splat Curling Up in Thermal Spray Coatings, *J. Therm. Spray Technol.*, 2006, **15**(4), p 531-536
25. M. Xue, S. Chandra, J. Mostaghimi, and H.R. Salimijazi, Formation of Pores in Thermal Spray Coatings Due to Incomplete Filling of Crevices in Patterned Surfaces, *Plasma. Chem. Plasma Process.*, 2007, **27**(5), p 647-657
26. H.B. Parizi, L. Rosenzweig, J. Mostaghimi, S. Chandra, T. Coyle, H. Salimi, L. Pershin, A. McDonald, and C. Moreau, Numerical Simulation of Droplet Impact on Patterned Surfaces, *J. Therm. Spray Technol.*, 2007, **16**(5-6), p 713-721
27. D.E. Wroblewski, R. Khare, and M. Gevelber, Solidification Modeling Plasma Sprayed TBC: Analysis of Remelt and Multiple Length Scales of Rough Substrates, *J. Therm. Spray Technol.*, 2002, **11**(2), p 266-275
28. S.N. Basu, G. Ye, R. Khare, B. McCandless, M. Gevelber, and D.E. Wroblewski, Dependence of Splat Remelt and Stress Evolution on Surface Roughness Length Scales in Plasma Sprayed Thermal Barrier Coatings, *Int. J. Refract. Met. Hard Mater.*, 2009, **27**, p 479-484
29. MatWeb, Material Property Data, 2008, 11/11/2008; Available from: <http://www.matweb.com/>
30. P.R. Munroe, The Application of Focused Ion Beam Microscopy in the Material Sciences, *Mater. Charact.*, 2009, **60**, p 2-13
31. S. Brossard, A.T.T. Tran, P.R. Munroe, and M.M. Hyland, Study of the Splat Formation for Plasma Sprayed NiCr on an Al5052 Substrate as a Function of Substrate Condition, *Surf. Coat. Technol.*, 2010, doi: [10.1016/j.surfcoat.2010.02.013](https://doi.org/10.1016/j.surfcoat.2010.02.013)
32. C.S. Giggins and F.S. Pettit, Oxidation of Ni-Cr-Al Alloys Between 1000 and 1200 °C, *J. Electrochem. Soc.*, 1971, **118**(11), p 1782-1790
33. M. Fukumoto, M. Shiiba, H. Kaji, and T. Yasui, Three-Dimensional Transition Map of Flattening Behavior in the Thermal Spray Process, *Pure Appl. Chem.*, 2005, **77**(2), p 429-442
34. X.Y. Jiang, Y. Wan, H. Herman, and S. Sampath, Role of Condensate and Adsorbates on Substrate Surface on Fragmentation of Impinging Molten Droplets During Thermal Spray, *Thin Solid Films*, 2001, **385**, p 132-141
35. C.-L. Li and J.-L. Li, Evaporated-Gas-Induced Splashing Model for Splat Formation During Plasma Spraying, *Surf. Coat. Technol.*, 2004, **184**, p 13-23
36. A.T.T. Tran and M.M. Hyland, The Role of Substrate Surface Chemistry on Splat Formation During Plasma Spray Deposition by Experiments and Simulations, *J. Therm. Spray Technol.*, 2010, **19**(1-2), p 11-23
37. S. Goutier, M. Vardelle, J.C. Labbe, and P. Fauchais, Alumina Splat Investigation: Visualization of Impact And Splat/Substrate Interface for Millimetre Sized Drops, *J. Therm. Spray Technol.*, 2010, **19**(1-2), p 49-55
38. H. Beck and H.-J. Güntherodt, *Glassy Metals*, Springer-Verlag, Berlin, 1983
39. S. Brossard, A.T.T. Tran, P.R. Munroe, and M.M. Hyland, Study of the Splat Formation for Plasma Sprayed NiCr on Aluminum Substrate as a Function of Substrate Condition, *Surf. Coat. Technol.*, 2010, **204**(16-17), p 2647-2656